

## COMPUTATIONAL SCREENING OF POTENT ANTI-INFLAMMATORY COMPOUNDS FOR HUMAN MITOGEN-ACTIVATED PROTEIN KINASE: A COMPREHENSIVE AND COMBINED IN SILICO APPROACH

BRIAN BASTO FRANCO, PANDIYARAJAN AGILANDESWARI, LAKSHMINARAYANAN KARTHIK\*

Precision Therapeutics Laboratory, Quick Is Cool, Aitele Research LLP, Bihar, India

\*Corresponding author: Lakshminarayanan Karthik; \*Email: [lnbioinfokarthik@gmail.com](mailto:lnbioinfokarthik@gmail.com)

Received: 20 Sep 2024, Revised and Accepted: 28 Oct 2024

### ABSTRACT

**Objective:** Inflammatory diseases have a serious impact on one's life and represent a diverse group of ailments stemming from various causes and presenting in various forms. p38 $\alpha$  of the mitogen-activated protein kinase family plays a crucial role in regulating inflammation, where the activation of this kinase initiates a cascade of events resulting in the production of proinflammatory mediators and cellular stress responses. In this context, attempts were made to identify potent small-molecule inhibitors of p38 $\alpha$  and assess their binding affinity through molecular docking studies.

**Methods:** From comprehensive reviews of several published reports, a few compounds, such as P38, P39, VPC00628, and N17, have shown substantial inhibitory activity toward p38 $\alpha$  at various concentrations. Hence, these four compounds were chosen as lead compounds, and small-molecule libraries were constructed on the basis of their structural similarity. Next, virtual screening docking was performed to investigate the inhibitory potency of the four libraries toward the p38 $\alpha$  isoforms (DFG-out and DFG-in), providing insights into their potential mechanisms of action.

**Results:** In addition, a comprehensive analysis of physicochemical and pharmacokinetic properties was also performed for the identified hits from each library. Our findings have shown that, compared with those of the p38 $\alpha$  DFG-in motif, the binding energies of the p38 $\alpha$  DFG-out motif are greater.

**Conclusion:** Furthermore, a few compounds from each library presented binding energies higher than those of their respective lead compounds, confirming their potential as novel therapeutic agents against inflammation.

**Keywords:** Inflammation, MAPK14, Virtual screening, Molecular docking, ADMET analysis

© 2024 The Authors. Published by Innovare Academic Sciences Pvt Ltd. This is an open access article under the CC BY license (<https://creativecommons.org/licenses/by/4.0/>) DOI: <https://dx.doi.org/10.22159/ijcpr.2024v16i6.6023> Journal homepage: <https://innovareacademics.in/journals/index.php/ijcpr>

### INTRODUCTION

Mitogen-activated protein kinase 14, otherwise referred to as MAPK14 or simply p38 $\alpha$ , plays an essential role in the cellular cascades that constitute the signaling events involved in the response to various extracellular stimuli. More particularly, it is genuinely a rate-limiting activator of immune responses, cell proliferation, differentiation, and apoptosis, as it reportedly assumes one of the central positions among the regulators of inflammatory pathways [1-3]. Its activation, as a result of various inflammatory mediators and stressors, leads to the phosphorylation of downstream effectors, controlling cellular behavior and gene expression in healthy and diseased states [4, 5]. The osmoregulatory protein kinases known as p38-MAPKs, or cytokine-suppressive anti-inflammatory drug-binding proteins, are triggered by many forms of cellular stress. Furthermore, mitogens only weakly activate them; nonetheless, endotoxins, proinflammatory cytokines, TNF- $\alpha$ , interleukin-1, osmotic shock, heat stress, or metabolic inhibitors such as sodium arsenite potentiate their responses [6]. Several published reports have indicated a strong correlation between the initiation of cellular inflammation and p38 $\alpha$  MAPK. Furthermore, the activation of p38 $\alpha$  MAPK can trigger the release of several proinflammatory proteins, such as TNF- $\alpha$  and IL-6 [7]. There are four isomers in the p38 group: p38 $\alpha$ , p38 $\beta$ , p38 $\gamma$ , and p38 $\delta$ . The cytoplasm and nuclei of quiescent cells contain all four isomers. They accumulate in the nuclei of cells following exposure to specific stressors [8]. On the other hand, some data indicate that following cell stimulation, active p38s may also be found in the cytoplasm [9].

Among the isomers, p38 $\alpha$  is the most expressed of the four and the most responsive to stress stimuli. They play a crucial role in inflammatory diseases and are associated with the etiology of several ailments, such as rheumatoid arthritis, inflammatory bowel disease, and cardiovascular disorders. The persistent synthesis of proinflammatory mediators and cytokines, which sustains chronic

inflammation and tissue damage, is facilitated by the dysregulated activation of MAPK14 [10]. Thus, p38 $\alpha$  has become a promising therapeutic target for identifying and developing new anti-inflammatory drugs to reduce the harmful consequences of dysregulated immune responses. However, a prevalent problem with current p38 $\alpha$  inhibitors is their toxic side effects. Though the abundance and low toxicity of natural compounds offer significant potential for developing p38 $\alpha$  inhibitors, only a few known natural compounds that target p38 $\alpha$  exist. For this reason, the search for potent anti-inflammatory agents that block p38 $\alpha$  has garnered much interest in the scientific community.

With advances in computer technology and chemical simulation, computational methods are widely used in drug development. Since conventional experimental screening approaches are laborious and time-consuming [11], virtual screening has emerged as a cost-effective alternative. This technique can significantly reduce the number of compounds that require additional experimental validation by screening a small number of potentially active compounds from many known or unknown compounds [12]. Hence, in the present study, attempts were made to identify compounds capable of modulating the activity of p38 $\alpha$ . By using various methods, such as lead compound-based library screening, virtual screening docking, and evaluation of physicochemical and drug-likeness properties, the results of this study lay the foundation for identifying potent anti-inflammatory compounds that target p38 $\alpha$  MAPK14.

### MATERIALS AND METHODS

The active site pocket of p38 $\alpha$  can adopt two different conformations, the "DFG-in" and "DFG-out" motifs, comprising aspartic acid, phenylalanine, and glycine. Owing to the presence of either of these motifs, the active site of p38 $\alpha$  is often referred to as having "open" or "closed" conformations. Furthermore, the presence of these motifs also helps in determining their functional form, where p38 $\alpha$  with the

DFG-in motif is generally assumed to be in the active form. In contrast, those with the DFG-out motif are considered inactive. Thus, the previously reported inhibitors are classified into two types: Type I (for the DFG-in motif) and Type II (for the DFG-out motif) [13]. On the basis of this observation, the following crystal structures of p38 $\alpha$  (PDB: 6HWT, DFG-out, and PDB: 3MGY, DFG-in) were chosen as the drug targets for performing virtual screening docking studies.

### Protein preparation

After retrieving the drug targets [14, 15] from the protein data bank and before virtual screening docking, the co-crystal ligands in the respective protein structures were removed permanently. In the next step, we added polar hydrogens to the protein structure and assigned Kohlman charges for each atom, ensuring accurate modeling of electrostatic interactions during the docking process. We also removed water molecules, other ligands, and any artifacts found in protein structures to simplify the docking process and reduce computational complexity.

### Screening of libraries

As mentioned earlier, the p38 MAPK family comprises four isoforms ( $\alpha$ ,  $\beta$ ,  $\gamma$ , and  $\delta$ ), among which p38 $\alpha$  is considered the primary isoform implicated in inflammatory responses [16]. Therefore, numerous studies have focused on developing orally active small-molecule inhibitors that target p38 $\alpha$  [17]. In one such similar study, the following compounds, 5-methyl-4-[2-methyl-5-[(2-morpholin-4-yl)pyridine-4-carbonyl]amino]anilino]-N-(1-phenylethyl)pyrrolo

[2,1-f][1,2,4]triazine-6-carboxamide, henceforth referred to as P38, and 5-methyl-4-[2-methyl-5-[(3-morpholin-4-yl)benzoyl]amino]anilino]-N-[(1S)-1-phenylethyl]pyrrolo[2,1-f][1,2,4]triazine-6-carboxamide, henceforth referred to as P39, were identified as potent inhibitors of p38 $\alpha$  [18]. Similarly, VPC00628, which was discovered within a DNA-encoded small-molecule library containing 12.6 million members and co-crystallized with p38 $\alpha$  (PDB: 5LAR) [19], and N17: 3-(4-methyl-1H-imidazol-1-yl)-N-[4-(pyridin-4-yloxy) phenyl] benzamide, which was co-crystallized with p38 $\delta$  (PDB: 5EKO) [20], has also shown substantial inhibitory activity against p38 $\alpha$  and p38 $\delta$ , respectively.

Furthermore, while X-ray crystallography studies of P38, P39, and VPC00628 with p38 $\alpha$  have revealed that these inhibitors bind to the DFG-out motif [18, 19], the crystal structure of the complex of N17 with p38 $\delta$  has shown that it is bound to the DFG-in motif [20]. However, irrespective of the position of the "Phe" residue in the DFG motif, all the reported inhibitors preferentially bind at the ATP pocket, as observed in their respective crystal structure complexes [20]. Hence, in the present study, "P38, P39, VPC00628, and N17" (fig. 1) were selected as the lead compounds for performing virtual screening docking against the DFG-out and DFG-in isoforms of p38 $\alpha$ . As a next step, a comprehensive similarity search was employed, where small-molecule compounds structurally similar to the lead compounds were searched in the PubChem and Binding databases. Among these repositories, compounds structurally similar to each of these lead compounds were retrieved in 3-D format for further virtual screening docking studies.

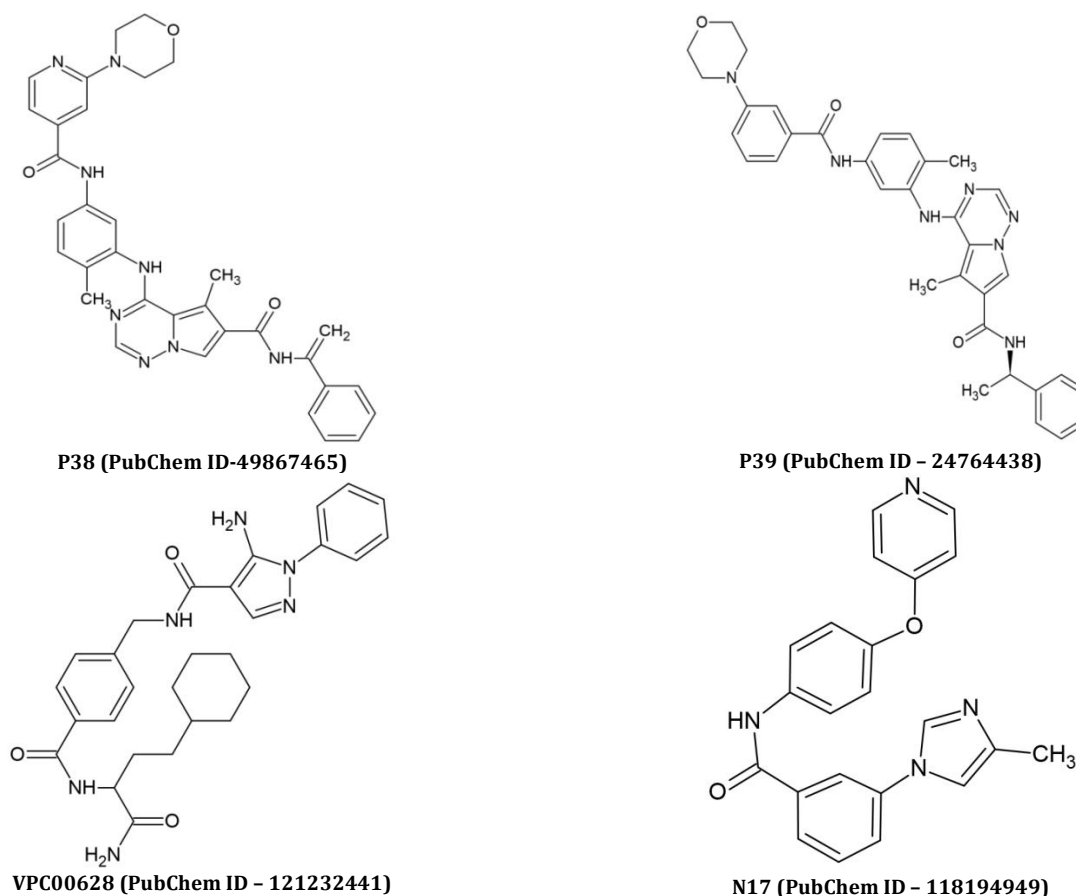


Fig. 1: 2D chemical representations of the four lead compounds

### Molecular docking using PyRx

Virtual screening docking was performed using AutoDock Vina in PyRx version 0.8 [21]. AutoDock Vina is a popular molecular docking program used to predict the binding orientation of ligands to a receptor (in this case, the protein). The 3-dimensional structures of

the chosen small-molecule libraries were downloaded from PubChem in ".sdf" file format and then converted to a "pdbqt" file via Open Babel (incorporated within PyRx software). To aid molecular docking, a three-dimensional grid box with an exhaustiveness value of eight was set up. This design allows the program to explore multiple conformations of the ligand in search of the best docking

position with high precision. The dimensions of the box were as follows: for p38 $\alpha$  DFG-out (PDB: 6HWT), size\_x = -11.6857 Å; size\_y = -4.4120 Å; size\_z = 17.9076 Å (XYZ dimension: 182×113×140 Å), and for p38 $\alpha$  DFG-in (PDB: 3MGY), size\_x = 44.5229 Å; size\_y = 30.3716 Å; size\_z = -18.6070 Å (XYZ dimension: 187×114×143 Å). During the docking procedure, ligands are treated as flexible entities, allowing them to adapt their conformations for optimal binding. Conversely, proteins are treated as rigid structures, maintaining their fixed conformation. The outcomes of the protein–ligand docking interactions were subsequently visualized and analyzed using ChimeraX software [22] and the Discovery Studio program [23], respectively.

#### Evaluation of physicochemical parameters – swissADME

For any drug discovery studies, predicting the physicochemical properties and the profile related to absorption, distribution, metabolism, excretion, and toxicity (ADMET) of the identified hits must be evaluated to minimize the unwanted side effects. In this context, we employed two well-known online tools: SwissADME [24] for assessment of physicochemical properties and pkCSM [25] for predictions related to ADMET. The objective of using these tools was to enhance the knowledge regarding the characteristics of the compounds. Analyzed for its wide range of analytical functionality, SwissADME was applied to assess molecular properties pertinent to the compounds of interest. Leveraging this tool, crucial parameters such as molecular weight, lipophilicity, and water solubility, among others, were elucidated, providing invaluable insights into the chemical nature of the compounds under investigation.

#### Evaluation of ADMET properties and toxicity predictions–pkCSM

pkCSM is a user-friendly, highly integrated online tool for estimating the pharmacokinetic profile and potential toxicity of compounds of interest. The SMILES notation of the top-ranked compounds was used for predicting critical ADMET features. The findings of these analyses provide essential insight into the pharmacological viability and potential safety concerns associated with the compounds identified in each library.

#### RESULTS

In this study, comprehensive virtual screening docking was performed with the pre-constructed libraries against the DFG-out and DFG-in isoforms of p38 $\alpha$ . In each library, the compounds were ranked on the basis of their binding affinity, where compounds observed with a larger negative value are generally considered to have higher binding energy and stronger binding affinity. In this context, the binding energies of the top ten inhibitor compounds obtained for each library against DFG-out p38 $\alpha$  are provided in table 1a. Briefly, for the "P38 and P39" libraries, the top-ranked compounds presented binding energies ranging from "-11.9 to -9.9 kcal/mol". For the other two libraries, "VPC00628" and "N17," the binding energies of the higher-ranked compounds were in the ranges of "-10.4 to -9.1 kcal/mol" and "-10.9 to -9.1 kcal/mol," respectively (table 1a). Among the chosen lead compounds, only P39 (24764438) was found in the top ten lists of compounds with higher binding energies in their respective libraries.

**Table 1a: Virtual screening docking of various compound libraries toward DFG-out p38 $\alpha$  (PDB: 6HWT)**

S. No.	P38 library	Binding energy (kcal/mol)	P39 library	Binding energy (kcal/mol)	VPC00628 library	Binding energy (kcal/mol)	N17 library	Binding energy (kcal/mol)
1	68393958	-11.9	44449750	-11.7	162659820	-10.4	58917248	-10.9
2	56676902	-11.6	44450065	-11.4	162644000	-10.3	122312628	-10.8
3	141653921	-11.1	141653921	-11.0	145994863	-10.0	122313753	-10.8
4	58780506	-11.1	167017847	-11.0	134143410	-9.8	122313762	-10.8
5	58780478	-10.9	58780590	-10.9	162673311	-9.8	122312656	-10.7
6	58780471	-10.8	58780518	-10.8	162670512	-9.6	122313885	-10.5
7	56673581	-10.6	24764438	-10.5	145994399	-9.5	122312997	-10.3
8	58780539	-10.6	58780478	-10.4	162674058	-9.4	122312996	-10.2
9	58780593	-10.6	68393958	-10.1	1041174	-9.2	122312275	-9.4
10	167528936	-10.4	58780471	-9.9	162648519	-9.1	122312845	-9.1

To evaluate the binding affinities of P38, VPC00628, and N17 individually, these three lead compounds, alongside various FDA-approved drugs, were docked to DFG-out p38 $\alpha$  (table 1b).

Interestingly, the results revealed that the binding energies of the existing drugs and lead compounds were relatively lower than those of the compounds in their respective libraries (table 1a).

**Table 1b: Virtual screening docking of lead compounds and existing drugs toward DFG-out p38 $\alpha$  (PDB: 6HWT)**

S. No.	Lead compounds	Binding energy (kcal/mol)	Existing drugs	Binding energy (kcal/mol)
1	P38	-10.1	PLX8394	-8.7
2	VPC00628	-8.9	Sorafenib	-8.7
3	N17	-8.9	Dabrafenib	-8.5
4			Ulixertinib	-8.5
5			Vemurafenib	-8.1
6			Alisertib	-8.1
7			Teriflunomide	-7.6
8			Simvastatin	-7.0

As performed for DFG-out, comprehensive virtual screening docking was also performed for DFG-in p38 $\alpha$ , where the binding energies obtained for the top ten inhibitor compounds from each library are provided in table 1c.

In contrast to the results observed for DFG-out, the docking simulations performed with DFG-in p38 $\alpha$  revealed that, along with P39 (24764438), the remaining two lead compounds, P38

(49867465) and N17 (118194949), were also among the top ten compounds in their respective libraries. Incidentally, with a binding energy of -10.1, P39 was observed as the highest-ranked compound in its corresponding library (table 1c). Furthermore, the molecular docking of VPC00628 and the above-mentioned existing drugs with DFG-in p38 $\alpha$  yielded binding energies that were moderately lower than those of the top-ranked compounds of all four libraries (table 1d).

Table 1c: Virtual screening docking of various compound libraries toward DFG-in p38 $\alpha$  (PDB: 3MGY)

S. No.	P38 library	Binding energy (kcal/mol)	P39 library	Binding energy (kcal/mol)	VPC00628 library	Binding energy (kcal/mol)	N17 library	Binding energy (kcal/mol)
1	167528936	-10.2	24764438	-10.1	162644000	-10.5	122312628	-10.6
2	56676902	-10.0	58780590	-10.0	162659820	-10.0	122312845	-9.2
3	56673581	-9.9	58780478	-9.9	162648519	-9.6	58917248	-9.2
4	58780478	-9.5	44450065	-9.8	145994863	-9.6	122312275	-9.0
5	58780593	-9.4	58780518	-9.5	162670512	-9.4	122312997	-8.8
6	141653921	-9.3	44449750	-9.5	162673311	-9.4	122313762	-8.7
7	58780506	-9.3	167017847	-9.5	162674058	-9.2	118194949	-8.5
8	49867465	-9.2	68393958	-9.3	134143410	-9.1	122312996	-8.5
9	68393958	-9.1	68374740	-9.2	145994399	-8.5	122312656	-8.5
10	58780471	-9.1	58780471	-9.2	1041174	-8.2	122313885	-8.3

Table 1d: Virtual screening docking of lead compounds and existing drugs toward DFG-in p38 $\alpha$  (PDB: 3MGY)

S. No.	Lead compounds	Binding energy (kcal/mol)	Existing drugs	Binding energy (kcal/mol)
1	VPC00628	-8.1	PLX8394	-9.0
2			Vemurafenib	-8.6
3			Dabrafenib	-8.5
4			Alisertib	-8.3
5			Sorafenib	-8.3
6			Ulixertinib	-8.1
7			Simvastatin	-8.0
8			Teriflunomide	-6.8

Overall, when the binding energies of the lead compounds were compared between Tables 1a and 1c, (i) the majority of the top-ranked compounds remained the same for both DFG-out and DFG-in, albeit with varying binding affinities, and (ii) collectively, the top-ranked compounds from the four libraries demonstrated substantial binding affinity toward DFG-out (table 1a) compared with that of DFG-in p38 $\alpha$  (table 1c). Henceforth, all further analyses, such as hydrogen bonding and nonbonding interactions and physicochemical and pharmacokinetic properties, were performed

only for the lead compounds listed in table 1a. In addition to possessing higher binding energies, the top-ranked compounds from the four libraries exhibited favorable hydrogen bonding and nonbonded interactions. In particular, most of the top-ranked compounds in each library interact with the critical active site residues Asp, 168, Phe 169, and Gly 170 (part of the DFG motif) through hydrogen bonding interactions. Similarly, these compounds also interact with nearby key residues (around the ATP binding pocket) through several nonbonded interactions (fig. 2a-2h).

Table 2a: Physicochemical parameters of the top-ranked compounds from the P38 library

S. No.	Compound ID	Mol. wt g/mol	HBA	HBD	TPSA ( $\text{\AA}^2$ )	Log P <sub>o/w</sub> (Consensus)	Drug likeness: Y(Yes)/N(No) (Lipinski rules)	Bioavailability
1	68393958	593.65	6	3	112.89	4.21	Y, 1 Violation	0.55
2	56676902	564.61	6	2	100.86	4.63	Y, 1 Violation	0.55
3	141653921	603.71	5	3	112.89	4.60	Y, 1 Violation	0.55
4	58780506	573.62	7	2	113.33	3.14	N, 2 Violation	0.17
5	58780478	607.68	6	3	112.89	4.62	Y, 1 Violation	0.55
6	58780471	572.63	7	3	116.13	2.85	N, 2 Violation	0.17
7	56673581	564.61	6	2	100.86	4.53	Y, 1 Violation	0.55
8	58780539	616.69	8	3	125.36	3.05	N, 2 Violation	0.17
9	58780593	607.68	6	3	112.89	4.70	Y, 1 Violation	0.55
10	167528936	617.70	7	2	143.87	3.01	N, 2 Violation	0.17
<b>Veber</b>			<b>Ghose</b>			<b>Egan</b>		<b>Muegge</b>
Yes			No			Yes		Yes
Yes			No			Yes		No
Yes			No			Yes		Yes
No			No			Yes		No
Yes			No			Yes		No
Yes			No			Yes		Yes
Yes			No			Yes		No
Yes			No			Yes		No
Yes			No			Yes		No
No			No			No		No

Collectively, these compounds are involved in hydrogen bonding and nonbonded interactions with the amino acid residues Ser 28, Pro 29, Val 30, Gly 31, Tyr 35, Gly 36, Val 38, Ala 40, Arg 49, Ala 51, Lys 53, Arg 67, Arg 70, Glu 71, Leu 75, Leu 104, Val 105, Thr 106, Leu 108, Gly 110, Ile 147, His 148, Arg 149, Lys 152, Ser 154, Asn 155, Asp 168, Phe 169, Gly 170, Leu 171, Ala 172, Tyr 323, Gln 325, Phe 327,

and Glu 328, which are located within the ATP binding pocket of DFG-out p38 $\alpha$ . In summary, the virtual screening docking results revealed that the top-ranked compounds from the P38, P39, VPC00628, and N17 libraries demonstrated promising binding affinities, indicating their potential as lead candidates for further optimization and development.

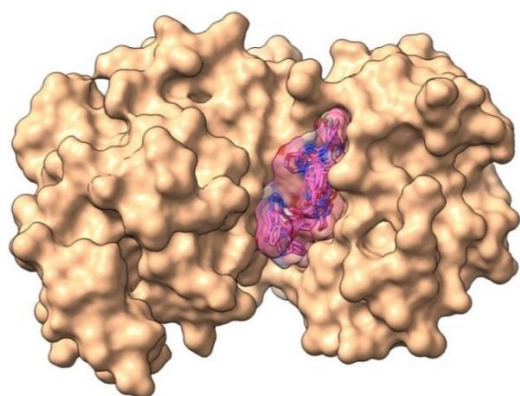


Fig. 2a

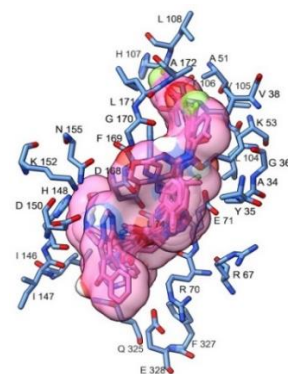


Fig. 2b

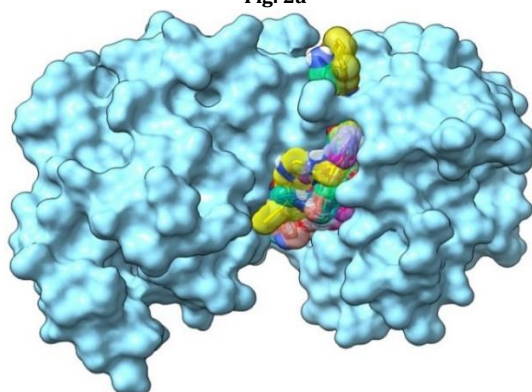


Fig. 2c

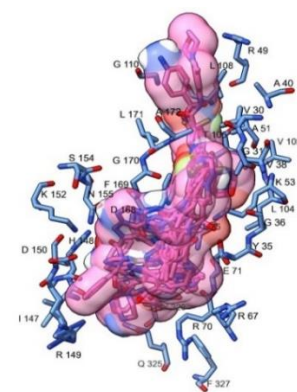


Fig. 2d

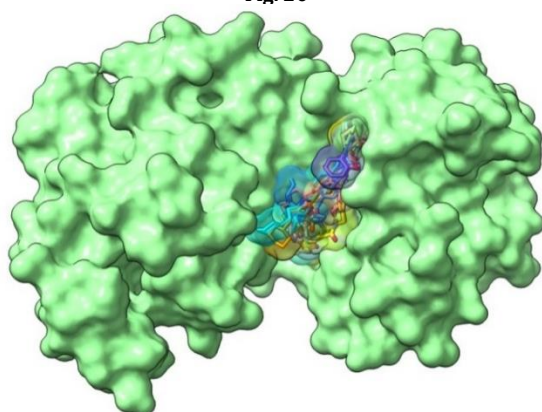


Fig. 2e

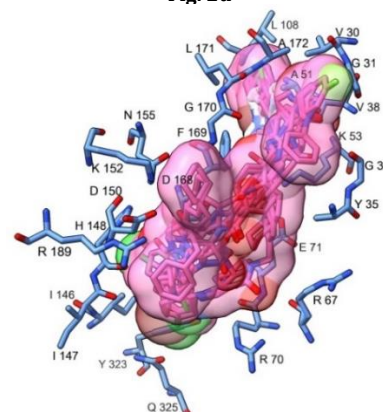


Fig. 2f

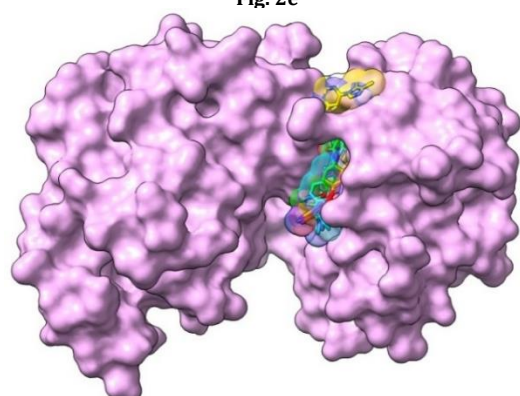


Fig. 2g

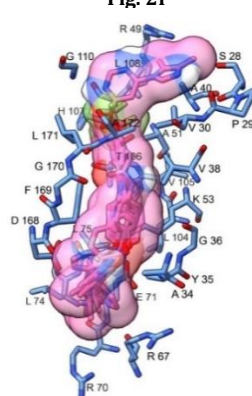


Fig. 2h

**Fig. 2:** 2a, 2c, 2e, and 2g superimposed image displaying the binding of the top-ranked compounds from the P38, P39, VPC00628, and N17 libraries, respectively, toward the active site (ATP binding) pocket of DFG-out p38 $\alpha$ . The image depicts the protein and top-ranked compounds via surface representation. In fig. 2b, 2d, 2f, and 2h, the top-ranked compounds from the four libraries are colored pink and shown in surface representation. To maintain clarity, the interactions are not shown here. Instead, the amino acid residues involved in the bonded and nonbonded interactions comprising van der Waals, pi-alkyl, and pi-sulfur interactions are colored blue and rendered in stick representation

### Evaluation of physicochemical and drug likeness

Physicochemical properties encompass various characteristics crucial for evaluating the suitability of a compound for drug development. Lipinski's rule of five has set the following thresholds to achieve optimal drug characteristics: molecular weight (MW)  $\leq$  500 g/mol, hydrogen bond donors (HBDs)  $\leq$  5, hydrogen bond acceptors (HBAs)  $\leq$  10, topological polar surface area (TPSA)  $\leq$  140 Å<sup>2</sup>, and average lipophilicity (Log Po/w)  $\leq$  5. Veber's rule adds criteria for bioavailability, emphasizing fewer rotatable bonds and a polar surface area  $\leq$  140. The Ghose filter highlights parameters such as MW (160–480 Da), LogP (-0.4–5.6), molar refractivity (40–130), and total number of atoms (20–70) for improved absorption prediction. The Egan rule outlines optimal bioavailability parameters: tPSA between 0 and 132 Å<sup>2</sup> and LogP between -1 and 6. Compounds within these ranges are more likely to be effectively absorbed, whereas those outside may face absorption challenges. Muegge's rule expands criteria, including MW (200–600), LogP (-2–5), polar surface area ( $\leq$  150), number of rings ( $\leq$  7), number of carbons ( $>$ 4), number of heteroatoms ( $>$ 1), rotatable bonds ( $\leq$  15), HBDs ( $\leq$  5), and HBAs ( $\leq$  10), differentiating between drug-like and

nondrug-like compounds. These parameters collectively aid in screening and selecting promising drug candidates.

Table 2a shows the physicochemical parameters of the lead compounds in the P38 library and their adherence to various drug-likeness standards. Although the compounds display a range of MWs that were found to exceed Lipinski's guidelines, on the basis of the expanded Muegge's filters, most of them were observed to be in the acceptable range. In addition to the preferred numbers of HBAs and HBDs, the TPSA values (100.86 Å<sup>2</sup> to 143.87 Å<sup>2</sup>) for all the compounds were also within the permissible limits. The lipophilicity values, represented by Log Po/w, range from 2.85 to 4.70, suggesting that all the compounds are likely capable of crossing the intestinal lipid membrane and remain soluble in the gastrointestinal tract as well. The bioavailability scores for all the compounds were either 0.17 or 0.55, indicating variable systemic circulation upon administration. Veber's and Egan's rules for the polar surface area are adhered to by most of the compounds, whereas Ghose's and Muegge's filters are partially fulfilled by some compounds. Overall, the data suggest a mixed profile of drug-likeness among the lead compounds from the p38 library, highlighting the need for further optimization and refinement.

**Table 2b: Physicochemical parameters of the top-ranked compounds from the P39 library**

S. No.	Compound ID	Mol. wt g/mol	HBA	HBD	TPSA (Å <sup>2</sup> )	Log P <sub>o/w</sub> (Consensus)	Drug likeness: Y(Yes)/N(No) (Lipinski rules)	Bioavailability
1	44449750	607.68	6	3	112.89	4.70	Y, 1 Violation	0.55
2	44450065	640.58	10	3	100.42	6.52	N, 2 Violation	0.17
3	141653921	603.71	5	3	112.89	4.60	Y, 1 Violation	0.55
4	167017847	609.69	6	3	112.89	4.14	Y, 1 Violation	0.55
5	58780590	608.67	7	3	125.78	4.01	N, 2 Violation	0.17
6	58780518	540.56	6	3	100.42	5.17	N, 2 Violation	0.17
7	24764438	589.69	5	3	112.89	4.33	Y, 1 Violation	0.55
8	58780478	607.68	6	3	112.89	4.62	Y, 1 Violation	0.55
9	68393958	593.65	6	3	112.89	4.21	Y, 1 Violation	0.55
10	58780471	572.63	7	3	116.13	2.85	N, 2 Violation	0.17
<b>Veber</b>			<b>Ghose</b>			<b>Egan</b>		<b>Muegge</b>
Yes			No			Yes		No
No			No			No		No
Yes			No			Yes		No
Yes			No			Yes		No
Yes			No			No		No
Yes			No			Yes		No
Yes			No			Yes		Yes
No			Yes			No		No
Yes			No			Yes		Yes

**Table 2c: Physicochemical parameters of the top-ranked compounds from the VPC00628 library**

S. No.	Compound ID	Mol. wt g/mol	HBA	HBD	TPSA (Å <sup>2</sup> )	Log P <sub>o/w</sub> (Consensus)	Drug likeness: Y(Yes)/N(No) (Lipinski Rules)	Bioavailability
1	162659820	726.71	4	3	125.59	5.29	N, 0 Violation	0.17
2	162644000	682.25	4	3	125.59	5.28	Y, 1 Violation	0.55
3	145994863	596.69	5	4	131.14	5.17	Y, 1 Violation	0.55
4	134143410	564.56	7	4	131.14	3.92	Y, 1 Violation	0.55
5	162673311	647.59	4	4	131.14	5.80	N, 2 Violation	0.17
6	162670512	614.68	6	4	131.14	5.31	Y, 1 Violation	0.55
7	145994399	584.75	4	4	131.14	4.98	Y, 1 Violation	0.55
8	162674058	736.50	4	4	131.14	5.90	N, 2 Violation	0.17
9	1041174	410.47	3	2	76.02	3.84	Y, 0 Violation	0.55
10	162648519	613.15	4	4	131.14	5.34	Y, 1 Violation	0.55
<b>Veber</b>			<b>Ghose</b>			<b>Egan</b>		<b>Muegge</b>
No			No			Yes		No
No			No			Yes		No
No			No			Yes		No
No			No			Yes		Yes
No			No			No		No
No			No			No		No
No			No			Yes		No
No			No			No		No
Yes			Yes			Yes		Yes
No			No			Yes		No

Table 2b shows the physicochemical parameters and adherence to various drug-likeness rules for lead compounds from the P39 library. As shown in the P38 library (table 2a), the MWs of the majority of the compounds in this library were >500 Da. However, when evaluated with Muegge's filter, their MWs were observed to be either within acceptable limits or marginally higher. However, the scores for the remaining parameters, such as HBAs, HBDs, and TPSA, were within the expected range. Furthermore, except for compound 2, the remaining compounds demonstrated substantial absorption through lipid membranes, as evidenced by their lipophilicity scores (2.85 to 5.17). Similarly, except for a few compounds, the bioavailability score for other compounds was 0.55, suggesting optimal systemic circulation upon administration. Veber's and Egan's rules are adhered to by most compounds, indicating favorable bioavailability, whereas Ghose's and Muegge's rules are partially fulfilled by some compounds. In general, the data indicate a heterogeneous affinity profile among the compounds in the P39 library, emphasizing the need for further optimization and refinement.

Table 2c presents the physicochemical parameters and adherence to various drug-likeness rules for lead compounds from the VPC00628 library. Most of the compounds presented relatively high MWs, ranging from 410.47 g/mol to 736.50 g/mol. However, as noted above in tables 2a and 2b, all the compounds in this library possess acceptable numbers of HBAs (3–7) and HBDs (2–4). The TPSA values range from 76.02 Å<sup>2</sup> to 131.14 Å<sup>2</sup>, which shows that all the compounds can typically have relatively high water solubility and, thus, favorable pharmacokinetic properties. The log Po/w values of all the lead compounds were marginally higher, suggesting that they are more likely to be dissolved in lipid environments. Except for a few compounds (1, 5, and 8), the bioavailability score was 0.55, confirming that the remaining compounds can exhibit optimal systemic circulation. For the additional filters, Veber, Ghose, and Muegge's rules were not met by most of the compounds, indicating challenges in terms of rotatable bonds and polar surface areas; the majority of them adhere to the criteria set by the Egan rule for good bioavailability. Overall, the data reveal that the lead compounds in the VPC00628 library require further optimization to improve their pharmacophore bioavailability.

**Table 2d: Physicochemical parameters of the top-ranked compounds from the N17 library**

S. No.	Compound ID	Mol. wt g/mol	HBA	HBD	TPSA (Å <sup>2</sup> )	Log P <sub>o/w</sub> (Consensus)	Drug likeness: Y(Yes)/N(No) (Lipinski rules)	Bioavailability
1	58917248	524.49	8	2	101.38	3.91	Y, 1 Violation	0.55
2	122312628	453.42	8	1	81.93	4.27	Y, 0 Violation	0.55
3	122313753	403.41	6	1	81.93	3.45	Y, 0 Violation	0.55
4	122313762	453.42	8	1	81.93	4.14	Y, 0 Violation	0.55
5	122312656	421.40	7	1	81.93	3.86	Y, 0 Violation	0.55
6	122313885	421.40	7	1	81.93	3.74	Y, 0 Violation	0.55
7	122312997	389.38	6	1	81.93	3.23	Y, 0 Violation	0.55
8	122312996	389.38	6	1	81.93	3.24	Y, 0 Violation	0.55
9	122312275	403.41	6	1	81.93	3.32	Y, 0 Violation	0.55
10	122312845	469.42	9	1	91.16	4.14	Y, 0 Violation	0.55
Veber		Ghose		Egan		Muegge		
Yes		No		No		Yes		
Yes		No		No		Yes		
Yes		Yes		Yes		Yes		
Yes		No		No		Yes		
Yes		Yes		Yes		Yes		
Yes		Yes		Yes		Yes		
Yes		Yes		Yes		Yes		
Yes		Yes		Yes		Yes		
Yes		Yes		Yes		Yes		
Yes		No		No		Yes		

In table 2d, the physicochemical parameters of the lead compounds from the N17 library are provided, along with their adherence to drug-likeness rules. All the compounds have MWs in the range of 389.38–524.49 g/mol, which is within the permissible limits of Lipinski's and Muegge's guidelines. The values of HBAs and HBDs, along with the TPSA parameters, were within their respective thresholds. The lead compounds also showed acceptable lipophilicity (log Po/w < 5), indicating that they can remain both lipophilic (efficiently cross the intestinal lipid membranes) and hydrophilic (displaying favorable solubility in the gastrointestinal tract). The bioavailability score for all the compounds was 0.55, indicating optimal systemic circulation upon administration. Veber's and Muegge's rules were satisfied by all the compounds, whereas Ghose's and Egan's filters were met by the majority of the compounds. On the basis of these data, it appears that the lead compounds sourced from the N17 library boasts a notably promising drug-likeness profile, underscoring their potential for advancement and thorough examination.

#### Pharmacological parameters and ADMET properties

Pharmacological parameters and ADMET properties are fundamental considerations in the drug development process and are essential for ensuring the efficacy and safety of potential therapeutic agents [26]. ADMET studies provide insights into how a chemical compound interacts within a living organism.

Pharmacokinetic assessments delve into the rates and pathways of absorption, distribution, metabolism, and excretion over time, which are pivotal for understanding a drug's behavior within the body.

The critical benchmarks in these studies include Caco2 permeability (>0.90 cm/s), which indicates effective human intestinal absorption, and intestinal absorption (IA > 30%), which is a promising marker of a compound. Skin permeability (>2.5) is assessed to gauge the likelihood of skin penetration, whereas blood–brain barrier (BBB) penetration (>0.3) is crucial for compounds that target the central nervous system (CNS). Additionally, CNS permeability (>2) is evaluated, with values indicating the potential for penetration into the CNS. Assessment of cytochrome P450 enzymes, such as CYP1A2 and CYP2C9, is essential because of their function in drug metabolism. Compounds that inhibit these enzymes may lead to drug–drug interactions or altered metabolism. Organic cation transporter 2 (OCT2), which is primarily found in the kidneys, is assessed for its impact on the renal clearance of drugs and endogenous compounds. Determining a compound's potential as a renal OCT2 substrate is crucial for understanding its disposition and potential for renal excretion.

Toxicology studies complement pharmacokinetic assessments by evaluating the safety profile of candidate compounds. Positive results in the AMES test indicate mutagenicity, raising concerns about carcinogenic potential. Hepatotoxicity assessments focus on

identifying drug-induced liver injury, which is a significant concern in drug development. Skin sensitization tests predict the likelihood of allergic reactions upon contact with the skin. The maximum recommended tolerated dose (MRTD) provides an estimate of the threshold for toxicity, where an MRTD > 0.477 log (mg/kg/day) indicates low toxicity and hence a good safety margin for the drug

compound. Oral rat acute toxicity (LD50) and chronic toxicity (LOAEL) studies aim to identify potential adverse effects and determine the lowest dose that produces observable toxicity. Collectively, these assessments guide the selection of promising drug candidates with optimal efficacy and safety profiles, facilitating their progression through preclinical and clinical development stages.

**Table 3a: Selected ADME properties of the top-ranked compounds from the P38 library**

Compound ID	Absorption			Distribution			Metabolism		Excretion	
	Caco2	IA	SP (log Kp)	BBB (log BB)	CNS (log PS)	CYP1A2 inhibitor	CYP2C9 inhibitor	TCL (log ml/min/kg)	Renal OCT2 substrate	
68393958	0.737	98.949	-2.735	-1.276	-3.212	No	Yes	-0.090	No	
56676902	1.166	100	-2.735	-0.726	-3.115	No	Yes	-0.005	No	
141653921	0.678	99.909	-2.735	-1.137	-2.159	No	Yes	0.042	No	
58780506	1.238	94.475	-2.736	-1.428	-3.446	No	Yes	-0.120	No	
58780478	0.677	100	-2.735	-1.315	-3.129	No	Yes	-0.160	No	
58780471	1.116	90.507	-2.735	-1.206	-3.490	No	Yes	0.507	No	
56673581	0.726	100	-2.735	-0.743	-3.162	No	Yes	-0.031	Yes	
58780539	0.975	90.826	-2.735	-1.432	-3.706	No	Yes	0.700	No	
58780593	1.262	100	-2.735	-1.353	-3.082	No	Yes	-0.134	No	
167528936	0.890	90.78	-2.735	-0.774	-3.646	No	Yes	0.356	No	

In table 3a, the selected lead compounds from the P38 library were subjected to a thorough assessment of their ADME properties and toxicity predictions to discern their pharmacokinetic behavior and safety profiles. Notably, all the compounds in this library presented favorable absorption parameters, confirming efficient intestinal absorption and Caco2 permeability. Similarly, all the compounds showed negligible skin penetration. In terms of the logBB and logPS

values, none of the lead compounds crossed the BBB or permeated the CNS. However, despite showing an affinity for CYP2C9, no compounds inhibited the other isoform, CYP1A2. The values obtained for the TCL parameter demonstrated that some compounds may have faster clearance than others. Except for compound 7, the remaining compounds cannot act as substrates for renal OCT2.

**Table 3b: Toxicity predictions for the top-ranked compounds from the P38 library**

Compound ID	AMES toxicity	Hepato-toxicity	Skin sensitization	Maximum tolerated dose	Oral rat acute toxicity (LD50)	Oral rat chronic toxicity (LOAEL)
68393958	No	Yes	No	0.511	3.420	1.625
56676902	No	Yes	No	0.398	3.184	1.439
141653921	No	Yes	No	0.495	3.397	1.598
58780506	No	Yes	No	0.270	2.965	1.191
58780478	No	Yes	No	0.495	3.432	1.549
58780471	No	Yes	No	0.404	3.025	1.540
56673581	No	Yes	No	0.571	3.354	1.696
58780539	No	Yes	No	0.419	2.999	1.548
58780593	No	Yes	No	0.326	3.262	1.409
167528936	No	Yes	No	0.419	2.755	1.241

According to the toxicity predictions in table 3b, all the lead compounds in the P38 library display promising safety profiles across multiple endpoints, suggesting minimal predicted toxicity. Although all the compounds had positive hepatotoxic effects, none had adverse AMES toxicity, indicating the absence of any possible mutagenic effects. All the compounds also had a negative effect on inducing allergic reactions upon skin exposure. With respect to the

MRTD, compounds 1, 3, 5, and 7 presented relatively high values, implying that these compounds have relatively high tolerances. In addition, all the compounds presented relatively high LD50 and LOAEL values, suggesting relatively low acute toxicity levels and that harmful effects can occur only at reasonably high doses. Collectively, these findings underscore their potential as candidates for further optimization and progression in drug development.

**Table 4a: Selected ADME properties of the top-ranked compounds from the P39 library**

Compound ID	Absorption			Distribution			Metabolism		Excretion	
	Caco2	IA	SP (log Kp)	BBB (log BB)	CNS (log PS)	CYP1A2 inhibitor	CYP2C9 inhibitor	TCL (log ml/min/kg)	Renal OCT2 substrate	
44449750	1.262	100	-2.735	-1.353	-3.082	No	Yes	-0.134	No	
44450065	1.080	100	-2.735	-1.680	-1.662	No	Yes	-0.584	No	
141653921	0.678	99.909	-2.735	-1.137	-2.159	No	Yes	0.042	No	
167017847	1.008	98.659	-2.737	-1.301	-2.998	No	Yes	0.000	No	
58780590	1.311	100	-2.735	-1.641	-3.522	No	Yes	-0.172	No	
58780518	1.135	98.874	-2.735	-1.365	-2.956	No	Yes	-0.270	No	
24764438	1.314	100	-2.735	-1.164	-2.208	No	Yes	0.062	No	
58780478	0.677	100	-2.735	-1.315	-3.129	No	Yes	-0.160	No	
68393958	0.737	98.949	-2.735	-1.276	-3.212	No	Yes	-0.090	No	
58780471	1.116	90.507	-2.735	-1.206	-3.490	No	Yes	0.507	No	

The analysis in table 4a highlights the ADME properties of the lead compounds from the P39 library, revealing several key features. All the compounds in this library demonstrated excellent absorption characteristics, confirming efficient intestinal absorption and robust Caco2 permeability. Additionally, none of these compounds penetrate the skin. According to the logBB and logPS values, most compounds do not cross the BBB or enter the CNS, except for compound 2, which

does show CNS permeability. With respect to metabolic interactions, all the compounds show affinity for CYP2C9; however, they do not inhibit the CYP1A2 isoform. The TCL parameter values suggest variability in the clearance rates of these compounds, indicating differences in how quickly they are metabolized and excreted. Moreover, none of the compounds act as substrates for the renal OCT2 transporter, suggesting a shared trait across the library.

**Table 4b: Toxicity predictions for the top-ranked compounds from the P39 library**

Compound ID	AMES toxicity	Hepato-toxicity	Skin sensitization	Maximum tolerated dose	Oral rat acute toxicity (LD50)	Oral rat chronic toxicity (Loael)
44449750	No	Yes	No	0.326	3.262	1.409
44450065	No	Yes	No	0.385	3.072	1.293
141653921	No	Yes	No	0.495	3.397	1.598
167017847	No	Yes	No	0.597	2.556	1.503
58780590	No	Yes	No	0.431	3.354	0.843
58780518	No	Yes	No	0.335	3.128	1.534
24764438	No	Yes	No	0.322	3.225	1.294
58780478	No	Yes	No	0.495	3.432	1.549
68393958	No	Yes	No	0.511	3.420	1.625
58780471	No	Yes	No	0.404	3.025	1.540

Table 4b provides a detailed examination of the toxicity profiles of the lead compounds in the P39 library, revealing promising results across multiple endpoints and suggesting minimal predicted toxicity. Despite all the compounds showing positive hepatotoxic effects, none were mutagenic, as indicated by the presence of negative AMES toxicity results. Moreover, none of the compounds induced allergic reactions

upon skin exposure. For MRTD, only compounds 3, 4, 8, and 9 presented relatively high values, implying potentially greater tolerance and adverse effects only at elevated doses. With respect to acute and chronic toxicity, all the compounds had reasonably high LD50 and LOAEL values, indicating a minimal risk of acute toxicity, with harmful effects most likely occurring at high doses.

**Table 5a: Selected ADME properties of the top-ranked compounds from the VPC00628 library**

Compound ID	Absorption			Distribution		Metabolism		Excretion	
	Caco2	IA	SP (log Kp)	BBB (log BB)	CNS (log PS)	CYP1A2 inhibitor	CYP2C9 inhibitor	TCL (log ml/min/kg)	Renal OCT2 substrate
162659820	1.018	87.534	-2.772	-1.137	-2.488	No	No	0.683	No
162644000	0.924	84.854	-2.741	-0.887	-2.171	No	Yes	-0.214	No
145994863	0.745	87.124	-2.804	-1.040	-2.544	No	No	0.844	No
134143410	0.496	76.107	-2.821	-1.286	-2.847	No	No	0.696	No
162673311	0.694	89.299	-2.778	-1.232	-2.322	No	No	0.628	No
162670512	0.697	87.301	-2.788	-1.186	-2.537	No	No	0.698	No
145994399	0.802	85.654	-2.822	-0.893	-2.591	No	No	1.01	No
162674058	0.703	88.771	-2.775	-1.248	-2.277	No	No	0.379	No
1041174	1.015	93.068	-3.458	-0.356	-2.38	No	No	0.747	No
162648519	0.743	88.123	-2.798	-1.063	-2.437	No	No	0.875	No

Table 5a displays the ADME properties of the lead compounds sourced from the VPC00628 library. Notably, although each compound in this library has shown remarkable intestinal absorption (IA>30%), very few compounds (1, 2, and 9) have displayed efficient Caco2 permeability. Moreover, it is worth mentioning that there is a complete absence of skin penetration for all the compounds. Moving on to the logBB and logPS values, none of the primary compounds

cross the BBB or permeate the CNS. Although all the compounds did not inhibit CYP1A2 or CYP2C9, compound 2 has an affinity for the CYP2C9 isoform. As the TCL parameter values are analyzed, interesting insights emerge that point to possible variations in clearance rates between compounds and their pharmacokinetic profiles. Furthermore, none of the compounds serve as substrates for renal OCT2, which underlines their distinct ADME characteristics.

**Table 5b: Toxicity predictions for the top-ranked compounds from the VPC00628 library**

Compound ID	AMES toxicity	Hepato-toxicity	Skin sensitization	Maximum tolerated dose	Oral rat acute toxicity (LD50)	Oral rat chronic toxicity (LOAEL)
162659820	No	Yes	No	-0.877	2.900	0.610
162644000	No	Yes	No	0.327	2.692	2.946
145994863	No	Yes	No	-0.678	2.916	0.663
134143410	No	Yes	No	-0.400	2.795	1.134
162673311	No	Yes	No	-0.699	2.937	0.346
162670512	No	Yes	No	-0.676	2.924	0.609
145994399	No	Yes	No	-0.675	2.891	0.766
162674058	No	Yes	No	-0.706	2.930	0.291
1041174	No	Yes	No	-0.147	2.826	1.126
162648519	No	Yes	No	-0.691	2.925	0.532

As shown in table 5b, the lead compounds from the VPC00628 library revealed promising safety profiles across various parameters, indicating minimal anticipated toxicity. All the compounds had positive hepatotoxic effects; however, none of them exhibited AMES toxicity, suggesting the absence of potential mutagenic effects. Additionally, there are no instances of allergenic reactions upon skin exposure to any of the compounds. With respect to the MRTD, none of

the compounds presented higher values, suggesting a restricted safety margin for all the compounds. Most compounds exhibited relatively high acute and chronic toxicity levels, except for compounds 5 and 8, which presented significantly lower LOAEL values. Nevertheless, the remaining lead compounds consistently suggest lower acute toxicity levels, implying that potential adverse effects may only emerge at relatively elevated doses.

**Table 6a: Selected ADME properties of the top-ranked compounds from the N17 library**

Compound ID	Absorption			Distribution			Metabolism		Excretion	
	Caco2	IA	SP (log Kp)	BBB (log BB)	CNS (log PS)	CYP1A2 inhibitor	CYP2C9 inhibitor	TCL (log ml/min/kg)	Renal OCT2 substrate	
58917248	0.575	87.804	-3.039	-1.248	-2.149	No	No	0.140	No	
122312628	0.895	87.436	-3.236	-0.943	-2.033	No	No	0.298	No	
122313753	0.937	89.909	-3.43	-0.651	-2.183	No	No	0.533	No	
122313762	0.895	87.436	-3.236	-0.943	-2.033	No	No	0.419	No	
122312656	0.928	89.108	-3.355	-0.796	-2.176	No	No	0.328	No	
122313885	0.833	93.605	-2.849	-1.380	-2.687	No	No	0.464	No	
122312997	0.938	90.111	-3.45	-0.657	-2.257	No	No	0.433	No	
122312996	0.938	90.111	-3.45	-0.657	-2.257	No	No	0.394	No	
122312275	0.960	90.744	-3.421	-0.669	-2.362	No	No	0.607	No	
122312845	0.903	87.183	-3.142	-1.127	-2.188	No	No	0.006	No	

Table 6a shows the ADME properties of the lead compounds in the N17 library. Each compound has favorable absorption traits, affirming efficient intestinal absorption and Caco2 permeability. Moreover, all the compounds exhibited minimal skin permeability, and no compound could breach either the BBB or the CNS. Similarly,

none of the compounds have shown affinity for the CYP1A2 or the CYP2C9 isoform. The values obtained for the TCL parameter revealed that there could be potential disparities in clearance rates among the compounds. Additionally, none of the compounds function as substrates for renal OCT2.

**Table 6b: Toxicity predictions for the top-ranked compounds from the N17 library**

Compound ID	AMES toxicity	Hepato-toxicity	Skin sensitization	Maximum tolerated dose	Oral rat acute toxicity (LD50)	Oral rat chronic toxicity (LOAEL)
58917248	No	Yes	No	-0.447	3.223	0.669
122312628	No	Yes	No	-0.271	3.369	0.709
122313753	No	Yes	No	-0.133	3.155	0.952
122313762	No	Yes	No	-0.271	3.369	0.709
122312656	No	Yes	No	-0.176	3.252	0.898
122313885	No	Yes	No	0.319	2.094	1.53
122312997	No	Yes	No	-0.075	3.142	1.011
122312996	No	No	No	-0.075	3.142	1.011
122312275	No	Yes	No	-0.106	3.101	1.036
122312845	No	Yes	No	-0.286	3.361	0.694

As shown in table 6b, a thorough investigation of the lead compounds included in the N17 library revealed robust toxicity profiles across diverse parameters. As observed in the other libraries, the lead compounds in this library had positive hepatotoxic effects. However, all the compounds showed no toxicity to AMES, confirming the absence of potential mutagenic effects. Similarly, all the compounds tended not to induce allergic reactions upon skin exposure. For the MRTD, all the compounds presented lower values, suggesting that they all possess only a narrow safety margin. With respect to acute and chronic toxicity, each compound presented much higher LD50 and LOAEL values, indicating markedly lower acute toxicity levels and suggesting that potential adverse effects would only occur at relatively higher doses.

## DISCUSSION

The traditional drug research and development process is often lengthy and increasingly inefficient, especially given the high financial inputs required. While *in silico* research is not capable of replacing experimental trials, it does provide a cost-effective and efficient method of identifying promising drug candidates, eventually helping in the development of novel medications [13]. Given this, the present study employed various computational techniques to screen and evaluate potent small-molecule inhibitors for the DFG-out conformation of the p38 $\alpha$  protein.

The study began by selecting lead compounds, including P38 and P39 analogs and VPC-00628 and N17 derivatives, on the basis of their documented potency and target enzyme interactions. The small-molecule libraries constructed from these lead compounds were subjected to virtual screening docking studies. While AutoDock Vina was used for molecular docking simulations, PyRx software was used for predicting binding orientations and interactions with the DFG-out p38 $\alpha$  protein to explore potential inhibitory mechanisms. Analyses of the docking results revealed that the binding energies obtained for the top-ranked compounds in all four libraries were significantly greater than those of several known anti-inflammatory drugs. All these compounds were then thoroughly evaluated for their physicochemical characteristics. Attention was paid to important parameters like MW, lipophilicity, aqueous solubility, and conformity to drug-likeness criteria. The in-depth analyses of the physicochemical properties revealed that, though the MWs of the top-ranked compounds from the P38, P39, and VPC00628 libraries were above 500 Daltons, all those compounds, together with the N17 library, were satisfactory for most of the other important parameters in terms of acceptable numbers of HBA, HBD, TPSA, lipophilicity, and drug-likeness criteria.

Similarly, ADMET predictions and toxicity evaluations were performed via pkCSM to investigate the absorption, distribution, metabolism, excretion, and toxicity profiles of the top-ranked

compounds in all four libraries. This analysis aimed to understand their pharmacokinetic behavior and safety margins. Profiling of absorption parameters of Caco2 permeability and intestinal absorption rates in each of the libraries showed that a significant number of compounds possessed the required permeability threshold of >0.90 cm/s and exceeded 30% intestinal absorption. The distribution characteristics, including the BBB and CNS permeability, suggest that none of the compounds from the four libraries tends to breach either the BBB or CNS. Metabolism profiles, as indicated by the P450 enzymes, confirmed that the top-ranked compounds from the four libraries could not inhibit CYP1A2; however, the compounds from the P38 and P39 libraries alone inhibited the CYP2C9 isoform of P450. The excretion profile comprising the TCL and renal OCT2 parameters indicated that, apart from demonstrating efficient clearance levels, no compounds from the four libraries acted as substrates for renal OCT2, thus reducing the risk of increased renal clearance.

On the toxicity front, evaluations such as the AMES test and hepatotoxicity assessments offered critical insights into genotoxicity and liver safety profiles, which are pivotal for clinical development. Although these compounds induce hepatotoxic effects, none have been found to induce mutagenic or allergic reactions. The safety margins were evaluated via parameters such as the MRTD, LD50, and LOAEL. Analysis of the MRTD scores revealed that the compounds from the P38 and P39 libraries presented higher tolerance levels than those from the VPC00628 and N17 libraries. However, the values obtained for the LD50 and LOAEL parameters revealed that all four libraries of compounds presented only lower acute toxicity levels.

## CONCLUSION

Overall, this research provides valuable insights into the molecular interactions, physicochemical properties, and pharmacokinetic profiles of lead compounds targeting p38 $\alpha$ , laying the groundwork for their advancement in preclinical and clinical studies. By leveraging a multidimensional approach encompassing computational modeling, physicochemical assessments, and toxicity predictions, we identified promising candidates to contribute to the development of innovative therapies targeting inflammatory pathways mediated by p38 $\alpha$  kinase. This work sets the stage for further optimization and refinement of lead compounds, with the ultimate goal of translating promising candidates into clinically viable therapeutic agents for the treatment of inflammatory disorders. The combined computational approaches described in this study provide insights for designing more analogs with reduced or less toxicity, which can be further utilized in treating patients with inflammatory diseases.

## ACKNOWLEDGEMENT

The authors would like to acknowledge the support offered by Dr. Monika Chauhan, PhD, Program Director and Dr. Shashank Taxak, CEO, at Aitele Research LLP for providing essential resources and creating an environment conducive to research.

## FUNDING

No funding was received for this study.

## AUTHORS CONTRIBUTIONS

Conceptualization: LK; Software: BB, AP; Investigation: BB, AP; Methodology: AP; Formal Analysis: BB; Writing-Original Draft Preparation: BB, AP; Writing-Review and Editing: BB, AP, LK; Supervision: LK.

## CONFLICT OF INTERESTS

The authors have no competing interests to declare.

## REFERENCES

- Falcicchia C, Tozzi F, Arancio O, Watterson DM, Origlia N. Involvement of p38 MAPK in synaptic function and dysfunction. *Int J Mol Sci.* 2020 Aug 6;21(16):5624. doi: [10.3390/ijms21165624](https://doi.org/10.3390/ijms21165624), PMID [32781522](https://pubmed.ncbi.nlm.nih.gov/32781522/).
- Yong HY, Koh MS, Moon A. The p38 MAPK inhibitors for the treatment of inflammatory diseases and cancer. *Expert Opin Investig Drugs.* 2009 Oct 23;18(12):1893-905. doi: [10.1517/13543780903321490](https://doi.org/10.1517/13543780903321490).
- Dong C, Davis RJ, Flavell RA. MAP kinases in the immune response. *Annu Rev Immunol.* 2002 Apr;20(1):55-72. doi: [10.1146/annurev.immunol.20.091301.131133](https://doi.org/10.1146/annurev.immunol.20.091301.131133), PMID [11861597](https://pubmed.ncbi.nlm.nih.gov/11861597/).
- Cuadrado A, Nebreda AR. Mechanisms and functions of p38 MAPK signalling. *Biochem J.* 2010 Aug 1;429(3):403-17. doi: [10.1042/BJ20100323](https://doi.org/10.1042/BJ20100323), PMID [20626350](https://pubmed.ncbi.nlm.nih.gov/20626350/).
- Han J, Sun P. The pathways to tumor suppression via route p38. *Trends Biochem Sci.* 2007 Aug 1;32(8):364-71. doi: [10.1016/j.tibs.2007.06.007](https://doi.org/10.1016/j.tibs.2007.06.007), PMID [17624785](https://pubmed.ncbi.nlm.nih.gov/17624785/).
- Umasuthan N, Bathige SD, Noh JK, Lee J. Gene structure molecular characterization and transcriptional expression of two p38 isoforms (MAPK11 and MAPK14) from rock bream (*Oplegnathus fasciatus*). *Fish Shellfish Immunol.* 2015 Nov 1;47(1):331-43. doi: [10.1016/j.fsi.2015.09.018](https://doi.org/10.1016/j.fsi.2015.09.018), PMID [26363230](https://pubmed.ncbi.nlm.nih.gov/26363230/).
- Kumar S, Boehm J, Lee JC. P38 MAP kinases: key signalling molecules as therapeutic targets for inflammatory diseases. *Nat Rev Drug Discov.* 2003 Sep;2(9):717-26. doi: [10.1038/nrd1177](https://doi.org/10.1038/nrd1177), PMID [12951578](https://pubmed.ncbi.nlm.nih.gov/12951578/).
- Haar ET, Prabhakar P, Liu X, Lepre C. Crystal structure of the p38 $\alpha$ -MAPKAP kinase 2 heterodimer. *J Biol Chem.* 2007 Mar 30;282(13):9733-9. doi: [10.1074/jbc.M611165200](https://doi.org/10.1074/jbc.M611165200), PMID [17255097](https://pubmed.ncbi.nlm.nih.gov/17255097/).
- Lee JC, Kumar S, Griswold DE, Underwood DC, Votta BJ, Adams JL. Inhibition of p38 MAP kinase as a therapeutic strategy. *Immunopharmacology.* 2000 May;47(2-3):185-201. doi: [10.1016/s0162-3109\(00\)00206-x](https://doi.org/10.1016/s0162-3109(00)00206-x), PMID [10878289](https://pubmed.ncbi.nlm.nih.gov/10878289/).
- DE Lorenzo A, Gratteri S, Gualtieri P, Cammarano A, Bertucci P, Di Renzo L. Why primary obesity is a disease? *J Transl Med.* 2019 May 22;17(1):169. doi: [10.1186/s12967-019-1919-y](https://doi.org/10.1186/s12967-019-1919-y), PMID [31118060](https://pubmed.ncbi.nlm.nih.gov/31118060/).
- Lin LT, Hsu WC, Lin CC. Antiviral natural products and herbal medicines. *J Tradit Complement Med.* 2014 Jan;4(1):24-35. doi: [10.4103/2225-4110.124335](https://doi.org/10.4103/2225-4110.124335), PMID [24872930](https://pubmed.ncbi.nlm.nih.gov/24872930/).
- Hou T, XU X. Recent development and application of virtual screening in drug discovery: an overview. *Curr Pharm Des.* 2004 Apr 1;10(9):1011-33. doi: [10.2174/1381612043452721](https://doi.org/10.2174/1381612043452721), PMID [15078130](https://pubmed.ncbi.nlm.nih.gov/15078130/).
- Vermani A, Kouznetsova VL, Tsigelny IF. New inhibitors of the p38 mitogen activated protein kinase: repurposing existing drugs with deep learning. *Biointerface Res Appl Chem.* 2021 Oct 18;12(4):5384-404. doi: [10.33263/BRIAC124.53845404](https://doi.org/10.33263/BRIAC124.53845404).
- Schehr M, Ianes C, Weisner J, Heintze L, Muller MP, Pichlo C. 2-Azo-2-diazocine thiazols and 2-azo-imidazoles as photoswitchable kinase inhibitors: limitations and pitfalls of the photo switchable inhibitor approach. *Photochem Photobiol Sci.* 2019 Jun 1;18(6):1398-407. doi: [10.1039/c9pp00010k](https://doi.org/10.1039/c9pp00010k), PMID [30924488](https://pubmed.ncbi.nlm.nih.gov/30924488/).
- Bukhtiyarova M, Karpusas M, Northrop K, Nambodiri HV, Springman EB. Mutagenesis of p38 $\alpha$  MAP kinase establishes key roles of Phe169 in function and structural dynamics and reveals a novel DFG-OUT state. *Biochemistry.* 2007 Apr 19;46(19):5687-96. doi: [10.1021/bi0622221](https://doi.org/10.1021/bi0622221), PMID [17441692](https://pubmed.ncbi.nlm.nih.gov/17441692/).
- Fearns C, Kline L, Gram H, Di Padova F, Zurini M, Han J. Coordinate activation of endogenous p38 $\alpha$ ,  $\beta$ ,  $\gamma$ , and  $\delta$  by inflammatory stimuli. *J Leukoc Biol.* 2000 May 1;67(5):705-11. doi: [10.1002/jlb.67.5.705](https://doi.org/10.1002/jlb.67.5.705), PMID [10811012](https://pubmed.ncbi.nlm.nih.gov/10811012/).
- Hynes J, Leftheri K. Small molecule p38 inhibitors: novel structural features and advances from 2002-2005. *Curr Top Med Chem.* 2005 Sep 1;5(10):967-85. doi: [10.2174/1568026054985920](https://doi.org/10.2174/1568026054985920), PMID [16178741](https://pubmed.ncbi.nlm.nih.gov/16178741/).
- Wroblewski ST, Lin S, Hynes J, WU H, Pitt S, Shen DR. Synthesis and SAR of new pyrrolo [2,1-f][1,2,4] triazines as potent p38 $\alpha$  MAP kinase inhibitors. *Bioorg Med Chem Lett.* 2008 Apr 15;18(8):2739-44. doi: [10.1016/j.bmcl.2008.02.067](https://doi.org/10.1016/j.bmcl.2008.02.067), PMID [18364256](https://pubmed.ncbi.nlm.nih.gov/18364256/).
- Petersen LK, Blakskjaer P, Chaikuad A, Christensen AB, Dietvorst J, Holmkvist J. Novel p38 $\alpha$  MAP kinase inhibitors identified from yocto Reactor DNA-encoded small molecule library. *Med.* 2016;7(7):1332-9. doi: [10.1039/C6MD00241B](https://doi.org/10.1039/C6MD00241B).
- Yurtsever Z, Patel DA, Kober DL, SU A, Miller CA, Romero AG. First comprehensive structural and biophysical analysis of

- MAPK13 inhibitors targeting DFG-in and DFG-out binding modes. *Biochim Biophys Acta*. 2016;1860:2335-44. doi: [10.1016/j.bbagen.2016.06.023](https://doi.org/10.1016/j.bbagen.2016.06.023), PMID [27369736](https://pubmed.ncbi.nlm.nih.gov/27369736/).
21. Dallakyan S, Olson AJ. Small molecule library screening by docking with PyRx. *Methods Mol Biol*. 2015;1263:243-50. doi: [10.1007/978-1-4939-2269-7\\_19](https://doi.org/10.1007/978-1-4939-2269-7_19), PMID [25618350](https://pubmed.ncbi.nlm.nih.gov/25618350/).
  22. Goddard TD, Huang CC, Meng EC, Pettersen EF, Couch GS, Morris JH. UCSF ChimeraX: meeting modern challenges in visualization and analysis. *Protein Sci*. 2018 Jan;27(1):14-25. doi: [10.1002/pro.3235](https://doi.org/10.1002/pro.3235), PMID [28710774](https://pubmed.ncbi.nlm.nih.gov/28710774/).
  23. Dassault systemes biovia, [Discovery Studio visualizer]. V20.1.0.19295. San Diego: Dassault Systemes; 2020.
  24. Daina A, Michielin O, Zoete V. Swiss ADME: a free web tool to evaluate pharmacokinetics drug likeness and medicinal chemistry friendliness of small molecules. *Sci Rep*. 2017 Mar 3;7(1):42717. doi: [10.1038/srep42717](https://doi.org/10.1038/srep42717), PMID [28256516](https://pubmed.ncbi.nlm.nih.gov/28256516/).
  25. Pires DE, Blundell TL, Ascher DB. PkcsM: predicting small molecule pharmacokinetic and toxicity properties using graph based signatures. *J Med Chem*. 2015 Apr 22;58(9):4066-72. doi: [10.1021/acs.jmedchem.5b00104](https://doi.org/10.1021/acs.jmedchem.5b00104), PMID [25860834](https://pubmed.ncbi.nlm.nih.gov/25860834/).
  26. Clark AM, Dole K, Coulon Spektor A, McNutt A, Grass GM, Freundlich JS. Open source bayesian models. 1. Application to ADME/Tox and drug discovery datasets. *J Chem Inf Model*. 2015 Jun 3;55(6):1231-45. doi: [10.1021/acs.jcim.5b00143](https://doi.org/10.1021/acs.jcim.5b00143), PMID [25994950](https://pubmed.ncbi.nlm.nih.gov/25994950/).